Central European Science Journals
www.cesj.com

Central European Journal of Physics
Central European Science Journals
CEJP 2 (2003) 246–257

Higher harmonics in the voltage on a superconducting wire carrying AC electrical current

Riccardo Tebano[1*] and Fedor Gömöry[2]

[1] *INFM, Istituto Nazionale per la Fisica della Materia, Dipartimento di Scienza dei Materiali dell'Università Statale di Milano-Bicocca, Milano, Italy*

[2] *Institute of Electrical Engineering, Slovak Academy of Sciences, Dubravska cest 9, Bratislava, Slovakia*

Received 6 November 2002; revised 24 February 2003

Abstract: The problem of determining the harmonic content in the voltage that appears on a superconducting wire carrying cosine-like AC current was resolved theoretically, using two approaches. First, the Fourier components of the voltage spectrum were found by numerical integration. Importance of individual terms was established, leading to two conclusions: a) it is the cosine component of the 3rd harmonic that represents the bulk of harmonic distortion, b) for the practical purposes it is sufficient to consider higher harmonics with $n \leq 7$. Then, the analytical formulas were derived. While for the sine components a general expression containing an infinite series was found, closed-form formulas were derived for the cosine components of the harmonics 1, 3, 5, 7. Consequences of the results to the experimental technique used to study the AC transport properties of superconductors are discussed.

Keywords: Type II superconductors, critical state, AC transport properties
PACS (2000): 74.60.Ge, 85.25.Am

1 Introduction

The shape of voltage signal from a superconductor carrying AC transport current bears significant information about the dynamics of magnetic flux penetration [1–3]. Due to the periodicity, it is natural to characterize the waveform by its harmonic spectrum. This is particularly convenient when the variation of current-carrying mechanisms (e.g.

* Present address: Pirelli Labs, Viale Sarca, 222, 20126 Milano, Italy

temperature) should be investigated [4,5]. Surprisingly, the formulas for higher harmonics in AC transport regime of superconductors have not been derived yet, in contrast to the case of AC magnetic experiments [6–10].

In our previous paper [11], we have shown how to express, across a complex equivalent inductance, the fundamental component of voltage on hard superconductor that transports AC current. Furthermore, both the electromagnetic energy dissipation and dispersion were described in a compact form.

Here we go further, deriving the higher harmonic components of such voltage. They could not contribute to energy-related characteristics like AC loss provided the AC current does not contain higher harmonics. However, they reflect the peculiarities of the voltage signal waveform. Our effort was motivated by the fact that the surface electrical field is the physical quantity currently investigated in standard AC transport experiments on superconducting samples. Extension of the commonly used technique of transport AC loss determination, based only on the separation of the in-phase fundamental harmonic component, to a more complex harmonic analysis offers, in our opinion, better description of the dynamics of magnetic flux penetration.

2 Time evolution of the electrical field

In this paper we investigate the waveform of the electrical field that has to be imposed to a wire from hard type II superconductor to make it carry the harmonic current of the form $I(t) = I_0 \cos \omega t$. An infinitely long, round wire, possessing perfect rotational symmetry with respect to its longitudinal axis, is considered in the following analysis. Distribution of the current density in the wire cross-section is supposed to follow the principles of the critical state model with constant value of the critical current density, j_c [12]. It has previously been shown how the AC current distributes in a round wire from hard superconductor, i.e. type II superconductor with flux pinning centres in its volume [13]. This process can be characterized as the magnetic flux penetration inwards the wire, with the penetration fronts in form of concentric circles that start from the surface, defined by the wire radius R. On the moving penetration front, the sign of local current density changes. Its value remains constant, given by the material's critical current density, j_c. This process happens twice in each AC cycle. For AC current amplitudes (I_0) lower than the wire's critical current ($I_c = \pi R^2 j_c$), a current-free zone remains near the wire axis where the electrical field is also zero. It is therefore often called the neutral zone. With the help of auxiliary variable $F = I_0/I_c$ one can describe the current density distribution in the first half of the cycle ($0 \le \omega t \le \pi$) as

$$j(r,t) = \begin{cases} -j_c & \text{for } R_t(t) \le r \le R \\ +j_c & \text{for } R_0 \le r \le R_t(t) \\ 0 & \text{for } r \le R_0 \end{cases} \tag{1}$$

where $R_0 = R\sqrt{1-F}$ is the radius of neutral zone and $R_t(t) = R\sqrt{1-(\cos\omega t - 1)F/2}$ is the radius of flux penetration front. In the second half of the cycle ($\pi \le \omega t \le 2\pi$)

$$j(r,t) = j(r, t-\pi/\omega) \tag{2}$$

and $R_t(t) = R\sqrt{1-(\cos\omega t + 1)F/2}$. The current distribution given by Eq.(1) generates on the wire surface ($r = R$) the magnetic field characterized by the vector potential

$$A_s(t) = -\frac{\mu_0 I_0}{4\pi}\left[\cos\omega t + \frac{1-F}{F}\ln(1-F) - \frac{2-F+F\cos\omega t}{F}\ln\left(1-\frac{F}{2}+\frac{F}{2}\cos\omega t\right)\right]$$

and a similar expression can be found also for the second half of the cycle.

Due to the existence of the neutral zone, the electrical field on the wire surface is entirely given by the time derivative of the vector potential, $E_s(t) = -\partial A_s(t)/\partial t$. Thus for the first half of the cycle $0 \le \omega t \le \pi$ we find that

$$E_s(t) = -\frac{\mu_0 I_0}{4\pi}\omega \sin\omega t \ln\left(1-\frac{F}{2}+\frac{F}{2}\cos\omega t\right) \tag{3}$$

while for $\pi \le \omega t \le 2\pi$ the surface electrical field will be

$$E_s(t) = -\frac{\mu_0 I_0}{4\pi}\omega \sin\omega t \ln\left(1-\frac{F}{2}-\frac{F}{2}\cos\omega t\right) \tag{4}$$

Comparing the last two expressions one finds that

$$E_s(r, t+\pi/\omega) = E_s(t) \tag{5}$$

The voltage waveform is given by the time-dependent dimensionless quantity

$$e_s(t) = E_s(t)\frac{4\pi}{\mu_0 I_0 \omega} \tag{6}$$

illustrated for a series of current amplitudes (i.e. with various parameter F) in Fig. 1. It is to be noted that for the case of an infinite slab, the shape of the waveform would not change with F [3]. However, experimental data [1,2] confirm the shape derived in [2] for a round wire.

3 Harmonic analysis of $E_s(t)$

The voltage waveform from Fig. 1 can be expressed by the series of Fourier components

$$e_s(t) = \sum_{n=1}^{\infty}\left[e_n^{''}\cos(n\omega t) + e_n^{'}\sin(n\omega t)\right] \tag{7}$$

where

$$e_n^{'} = \frac{1}{\pi}\int_0^{2\pi} e_s(t)\sin(n\omega t)\,d\omega t \tag{8}$$

$$e_n'' = \frac{1}{\pi} \int_0^{2\pi} e_s(t) \cos(n\omega t)\, d\omega t \tag{9}$$

Because of the symmetry (5), only odd harmonics are expected. This conclusion has been supported by experimental data [4] as well. When we performed the above integrations in numerical way, the results were obtained that for n up to 7, and are plotted in Fig. 2 by symbols. All the components except e_1'' (this is that one responsible for the dissipation) bear negative sign, thus they were multiplied by -1 to allow for logarithmic scale. From the sine components, only that fundamental one is significant at low current amplitudes. Higher sine components increase rapidly when I_0 approaches I_c, and eventually at $F \to 1$, when $I_0 \approx I_c$, they reach the level quite close to that of the cosine components. Thus, for low current amplitudes (i.e., low F) the magnitude of any higher harmonic is essentially given by its cosine component. However, from Fig. 2 one can see that at the current amplitudes up to $I_0 \approx I_c/2$, the slope of all the cosine components is equal and corresponding to the second power of the AC current: $e_n''\big|_{F \ll 1} \propto F^2$. Due to this, at low currents the content of harmonics does not change with AC current amplitude, maintaining the relations presented in Table 1. As the reference quantity, the fundamental cosine component was chosen in this comparison. This is because it could be experimentally better defined than the sine component that in practice cannot be clearly distinguished from a parasitic voltage induced in the signal leads. We see that the bulk of higher harmonic generation is described by the third harmonic component. Our result for the 3rd harmonics is in agreement with the result of numerical finite-element computation [14].

The significance of the 3rd harmonic illustrates Fig. 3, where the original waveform calculated for $F = 0.1$ is compared with two substitutions generated by finite number of harmonic constituents. Fair agreement is reached already by the insertion of the third harmonic, and further addition of the 5th and 7th harmonics results in very good waveform description. Nevertheless, for large currents, the higher harmonics cease rather slowly, resembling the Gibbs problem due to sharp edges of the waveform at $t = 0$ and $t = \pi/\omega$, respectively. This is illustrated in Fig. 4 where the same comparison is presented for $F = 1$. This is, however, an exceptional situation, and for most current amplitudes the use of the first seven harmonics is sufficient.

The problem of finding analytical solution for the integrals (8)–(9) for practical purposes can be therefore restricted to $n \leq 7$. Detailed derivation of analytic expressions for the Fourier components (8)–(9) is explained in the Appendix, here the summary of results is given. We found that only the expressions for cosine components exhibit true analytical form. For the sake of completeness, let us start with the cosine component of the fundamental harmonic:

$$e_1'' = \frac{4}{\pi F^2} \left[F\left(1 - \frac{F}{2}\right) + (1 - F)\ln(1 - F) \right] \tag{10}$$

This result could be also easily derived from the classical paper of Norris [13]. The cosine components for $n = 3, 5$ and 7 were found as

$$e_3'' = \frac{2}{3\pi F^4} \left[F(F-2)\left(F^2 + 24F - 24\right) - 6(F-1)\left(F^2 - 8F + 8\right)\ln(1 - F) \right] \tag{11}$$

$$e_5'' = \frac{2}{45\pi F^6}\left[\begin{array}{c} F\left(F-2\right)\left(7F^4+440F^3-4280F^2+7680F-3840\right)+ \\ -30\left(F-1\right)\left(3F^4-72F^3+328F^2-512F+256\right)\ln\left(1-F\right)\end{array}\right] \tag{12}$$

$$e_7'' = \frac{4}{630\pi F^8}\left[\begin{array}{c} F\left(F-2\right)\left(\begin{array}{c}29F^6+3472F^5-84112F^4+483840F^3+ \\ -1048320F^2+967680F-3225600\end{array}\right)+ \\ -210\left(F-1\right)\left(\begin{array}{c}3F^6-144F^5+1424F^4-5632F^3+ \\ +10496F^2-9216F+3072\end{array}\right)\ln\left(1-F\right)\end{array}\right] \tag{13}$$

As one can see, the limitation to the first 7 harmonics is conformal also with the requirement of practical applicability of the analytic results. Let us now revert to the sine components. For the first sine component we found

$$e_1' = \ln\left(1-\frac{F}{2}\right) - \sum_{k=1}^{\infty}\frac{(2k-1)!!}{2^{k+1}k\left(k+1\right)!}\left(\frac{F}{2-F}\right)^{2k} \tag{14}$$

This result is a simpler form of our previous equivalent inductance formula (6) in [11]. The sine components for $n = 3, 5$ and 7 were found as

$$e_3' = -3\sum_{k=1}^{\infty}\frac{(2k-1)!!}{2^{k+1}k\left(k+2\right)!}\left(\frac{F}{2-F}\right)^{2k} \tag{15}$$

$$e_5' = -5\sum_{k=1}^{\infty}\frac{(k-1)\left(2k-1\right)!!}{2^{k+1}k\left(k+3\right)!}\left(\frac{F}{2-F}\right)^{2k} \tag{16}$$

$$e_7' = -7\sum_{k=1}^{\infty}3\frac{(k-2)\left(k-1\right)\left(2k-1\right)!!}{2^{k+1}k\left(k+4\right)!}\left(\frac{F}{2-F}\right)^{2k} \tag{17}$$

It is possible to express the sine component for $n > 3$ in the general form

$$e_n' = -n\sum_{k=1}^{\infty}\frac{(2k-1)!!}{2^{k+1}k\left(k+\frac{n+1}{2}\right)!}\left(\frac{F}{2-F}\right)^{2k}\prod_{i=1}^{\frac{n-3}{2}}\left(k-i\right) \tag{18}$$

In all the previous formulas the symbol $(2k-1)!!$ stands for the product of the odd numbers $1 \times 3 \times 5 \times \ldots (2k-1)$.

Plots of these expressions are given in Fig. 2 by lines. The differences with respect to the values obtained by numerical integration are only on the level of calculation precision.

4 Discussion of results

Our results give quantitative description of the generally expected phenomena of non-harmonic voltage generation on a wire of hard superconductor carrying sinusoidal transport current. The formulas (10)–(18) do not depend on the wire dimensions. Further, the angle frequency of AC current, ω, appears as a pre-factor in the formula (6) for electrical field, as well as the amplitude of the current, I_0. Thus, the waveform of electrical field, e_s, is entirely determined by only one independent variable: the ratio F between the AC current's amplitude and the wire's critical current, I_c. This means the previous formulas are rather general and applicable to wide range of cases. We would like to underline two important consequences of our results.

The first consequence regards the measurement of superconductor's properties in AC transport conditions. At the present time, it commonly means the detection, with the help of a pair of voltage taps soldered to the wire surface, of fundamental voltage component in phase with transport current. The reason is that the AC loss, i.e. the electromagnetic energy converted in heat, can be determined in this way. In such procedure, only the information about e_1'' defined above is extracted from the measured signal. In the cases when the "loss behaviour" did not appear in agreement with theoretical predictions, several phenomena have been proposed to contribute to the observed losses. Most of them are of linear eddy-current like in nature, with no contribution to higher harmonics of the voltage signal [15,16]. This means they do not affect our predicted results of the harmonic composition of that part of the voltage that is linked with irreversible flux penetration into the superconductor bulk. Compliance with our results for higher harmonics would also indicate that the critical state model with constant j_c is appropriate in description of the flux dynamics in given wire, and vice versa; the deviation of observed harmonic composition from our predictions would mean that a correction to the theoretical model is necessary. Constant j_c can be achieved by superimposing a DC field much larger than that produced by transport current on a perfectly uniform wire. In this case, a deviation from the harmonic behaviour predicted here would point towards a radial inhomogeneity of j_c. And, if the harmonic pattern would change at DC field removal, it is the $j_c(B)$ dependence that could not be more neglected. We observed slightly lower content of higher harmonics with respect to that calculated here, when experimenting without DC superimposed field on wires from high temperature superconductor [17].

The second consequence regards the experimental technique of studying the AC transport properties of superconducting wires as well, though now it does not concern the measured voltage, but that furnished by the power supply. The current circuit does always make contact with the sample on its surface. This means that the non-harmonic voltage drop (3)–(5) must be present at the current leads to secure that the current in the wire is harmonic. Importance of maintaining a harmonic waveform of the current flowing in the sample is crucial; otherwise, the experimental conditions are no more defined, and any comparison with theoretical predictions or other results becomes defined. One can see in Fig. 2 how rich the harmonic content is when the AC current amplitude is approaching Ic. Therefore, checking the harmonic purity of the current should be highly recommended in these conditions.

5 Conclusions

We have analysed the harmonic content of the voltage that appears on a superconducting wire carrying harmonic AC current. The problem of finding the Fourier components was resolved by two different approaches. We first determined the Fourier components of the voltage spectrum by numerical integration of the product of the voltage and the respective harmonic function. To reach more general results, we derived the analytical formulas for at least some significant terms. Because the waveform symmetry inhibits the even terms, only those with odd order number were regarded.

We found that the cosine component of the 3$^{\text{rd}}$ harmonic represents significant part of the harmonic distortion. The sine components, except the fundamental one that remains at any condition the largest component, are negligible in comparison to the cosine components starting from low currents up to around the half of the critical current. The decrease of Fourier coefficients is rather slow at the currents with amplitudes quite close to I_c, but for the rest of the current range one could limit the analysis to the harmonics with $n \leq 7$. We derived the analytical formulas for all the sine components that represent a general expression containing an infinite series, and for the cosine components with $n = 1, 3, 5, 7$ that have the form of analytical expressions with rapidly increasing complexity.

Our results allow to check the behaviour of superconducting wire by an analysis that is more complex than the single AC loss evaluation generally used at the present time.

Acknowledgment

The authors acknowledge the financial support of the European Commission (projects G3RD-CT2000-0239 Q-Secrets and SCENET) and Slovak Grant Agency VEGA.

6 Appendix

The details of deriving of the expressions for the Fourier's coefficients, defined by the equations (8), (9) are given in the following. Because of the symmetry (5), only odd harmonics are expected. Taking into account also the symmetry of the trigonometric functions, the expressions can be written as:

$$e_n' = \begin{cases} \frac{2}{\pi} \int_0^{\pi} e_s(t) \sin(n\omega t)\, d\omega t & n \text{ odd} \\ 0 & n \text{ even} \end{cases}$$

$$e_n'' = \begin{cases} \frac{2}{\pi} \int_0^{\pi} e_s(t) \cos(n\omega t)\, d\omega t & n \text{ odd} \\ 0 & n \text{ even} \end{cases}$$

From the De Moivre's formula it is possible to get the following expressions for sine and cosine of n times the given angle:

$$\cos(n\omega t) + i\sin(n\omega t) = (\cos\omega t + i\sin\omega t)^n$$

and then:

$$\begin{cases} \cos(n\omega t) = \sum_{\substack{l=1 \\ l \text{ even}}}^{n} \binom{n}{l} (-1)^{\frac{l}{2}} \sin^l \omega t \cos^{n-l}\omega t \\ \sin(n\omega t) = \sum_{\substack{l=1 \\ l \text{ odd}}}^{n} \binom{n}{l} (-1)^{\frac{l-1}{2}} \sin^l \omega t \cos^{n-l}\omega t \end{cases}$$

where the brackets represent the binomial coefficients.

For the real part e_n'' the integration doesn't present any difficulty. It is enough to perform the substitution $y = \cos\omega t$ and $dy = -\omega\sin\omega t$ to obtain

$$e_n'' = \frac{2}{\pi}\int_{-1}^{1} \ln\left(1 - \frac{F}{2} + \frac{F}{2}x\right) P_n''(x)\,dx$$

where $P_n''(x)$ is an n degree polynomial of x:

$$P_n''(x) = \begin{cases} x & \text{for } n = 1 \\ 4x^3 - 3x & \text{for } n = 3 \\ 16x^5 - 20x^3 + 5x & \text{for } n = 5 \\ 64x^7 - 112x^5 + 56x^3 - 7x & \text{for } n = 7 \end{cases}$$

Such expressions are easily computed with the help of integrating by parts, and the results lead to the expressions (10)–(13).

The computation of the sine components of the Fourier expansion presents more difficulties. The first step is to make the substitution $\omega t = x$ and $d\omega t = dx$, then to rewrite and expand the ln in the expression for the surface electrical field as follows:

$$\begin{aligned} \ln\left(1 - \frac{F}{2} + \frac{F}{2}\cos x\right) &= \ln\left(1 - \frac{F}{2}\right) + \ln\left(1 + \frac{F}{2-F}\cos x\right) \\ &= \ln\left(1 - \frac{F}{2}\right) + \sum_{n=1}^{\infty} \frac{(-1)^{n+1}}{n}\left(\frac{F}{2-F}\right)^n \cos^n x \end{aligned}$$

The expression for the sine components, with even n, in the Fourier's expansion will be then:

$$\begin{aligned} e_n' = {} & \frac{2}{\pi}\ln\left(1 - \frac{F}{2}\right)\int_0^{\pi} P_n'(\cos x)\sin^2 x\,dx \\ & -\frac{2}{\pi}\sum_{\substack{n=2 \\ n \text{ even}}}^{\infty} \frac{1}{n}\left(\frac{F}{2-F}\right)^n \int_0^{\pi} P_n'(\cos x)\sin^2 x\cos^n x\,dx \end{aligned}$$

where

$$P_n'(\cos x) = \begin{cases} 1 & \text{for } n=1 \\ 4\cos^2 x - 1 & \text{for } n=3 \\ 16\cos^4 x - 12\cos^2 x + 1 & \text{for } n=5 \\ 64\cos^6 x - 80\cos^4 x + 24\cos^2 x - 1 & \text{for } n=7 \end{cases}$$

At this stage it is possible to perform the computation taking advantage of another useful relation derived from Handbook of Mathematical Functions, (Ed. By M. Abramowitz and I.A. Stegun):

$$\int_0^\pi \sin^2 x \cos^{2k} x dx = \frac{(2k-1)!!}{2^k (k+1)!} \frac{\pi}{2}$$

The result of this computation are the expressions (14)–(18).

References

[1] M. Polák, I. Hlásnik, S. Fukui, N. Ikeda, O. Tsukamoto: "Self-field effect and current-voltage characteristics of a.c. superconductors", *Cryogenics*, Vol. 34, (1994), pp. 315.

[2] S.P. Ashworth: "Measurements of AC losses due to transport current in bismuth superconductors", *Physica*, Vol. C 229, (1994), pp. 355.

[3] A.N. Ulyanov: "Transport of alternating current and direct current by hard superconductors. critical and resistive state", *J. Appl. Phys*, Vol. 85, (1999), pp. 3726.

[4] T. Yamao, M. Hagiwara, K. Koyama, M. Matsuura: "Intergrain ordering of a superconductive ceramic of $YBa_2Cu_4O_8$ at zero external magnetic field", *J. Phys. Soc. Jpn.*, Vol. 68, (1999), pp. 871.

[5] A.M. Grishin, V.N. Korenivski, K.V. Rao, A.N. Ulyanov: "High-frequency harmonic generation by $Bi_2Sr_2Ca_2Cu_3O_y$ ceramic carrying alternating transport current", *Appl. Phys. Lett*, Vol. 65, (1994), pp. 487.

[6] L. Ji, H. Sohn, G.C. Spalding, C.J. Lobb M. Tinkham: "Critical-state model for harmonic generation in high-temperature superconductors", *Phys. Rev.*, Vol. B 40, (1989), pp. 10 936.

[7] T. Ishida and R.B. Goldfarb: "Fundamental and harmonic susceptibilities of $YBa_2Cu_3O_{7-\delta}$", *Phys. Rev.*, Vol. B 41, (1990), pp. 8937.

[8] P. Fabbricatore, S. Farinon, G. Gemme, R. Musenich, R. Parodi, B. Zhang: "Effects of fluxon dynamics on higher harmonics of ac susceptibility in type-II superconductors", *Phys. Rev.*, Vol. B 50, (1994), pp. 3189.

[9] M. Polichetti, M.G. Adesso, T. Di Matteo, A. Vecchione, S. Pace: "Detection of flux creep regime in the AC susceptibility curves by using higher harmonic response", *Physica*, Vol. C 332, (2000), pp. 378.

[10] A. Crisan, A Iyo, Y. Tanaka, M. Hirai, M. Tokumoto, H. Ihara: "Superconducting properties from AC susceptibility and harmonic generation in $CuBa_2Ca_3Cu_4O_y$", *Physica*, Vol. C 353, (2001), pp. 227.

[11] F. Gömöry and R. Tebano: “Low frequency impedance of a round cylindrical wire”, *Physica*, Vol. C 310, (1998), pp. 116.

[12] C.P. Bean: “Magnetization of hard superconductors”, *Rev. Mod. Phys.*, Vol. 36, (1964), pp. 31.

[13] W.T. Norris: “Calculation of hysteresis losses in hard superconductors carrying ac: isolated conductors and edges of thin sheets”, *J. Phys.*, Vol. D 3, (1970), pp. 489.

[14] E. Martinez, T.J. Hughes, Y. Yang, C. Beduz, L. A. Angurel: “Measurement of AC losses in textured polycrystalline Bi-2212 thin rods”, *IEEE Trans. Appl. Superconductivity*, Vol. 9, (1999), pp. 805.

[15] K.-H. Müller and K.E. Leslie: “Self-field AC loss of Bi-2223 superconducting tapes”, *IEEE Trans. Appl. Superconductivity*, Vol. 7, (1997), pp. 306.

[16] R. Tebano, A. Melini, R. Mele, G. Coletta: “Edddy current loss in Ag-sheathed BSCCO tapes in the AC transport regime”, *IEEE Trans. Appl. Superconductivity*, Vol. 11, (2001), pp. 2757.

[17] F. Gömöry, R. Tebano, J. Souc and S. Farinon: “Generation of Higher Harmonics in Voltage on Superconducting Wire Carrying Cosine-like AC Current”, *IEEE Trans. Appl. Superconductivity*, Vol. 13, (2003), accepted for publication.

n	3	5	7	9	11
$\frac{\sqrt{(e'_n)^2+(e''_n)^2}}{e''_1}$	0.6	0.144	0.067	0.039	0.026

Table 1 Relative magnitude of harmonic components at low currents

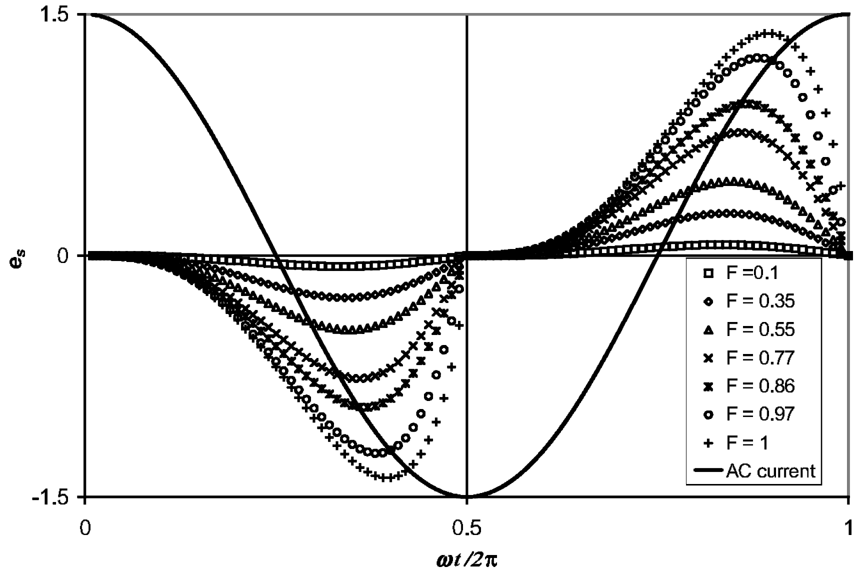

Fig. 1 Waveform of the surface voltage at different values of the ratio $F = I_a/I_c$

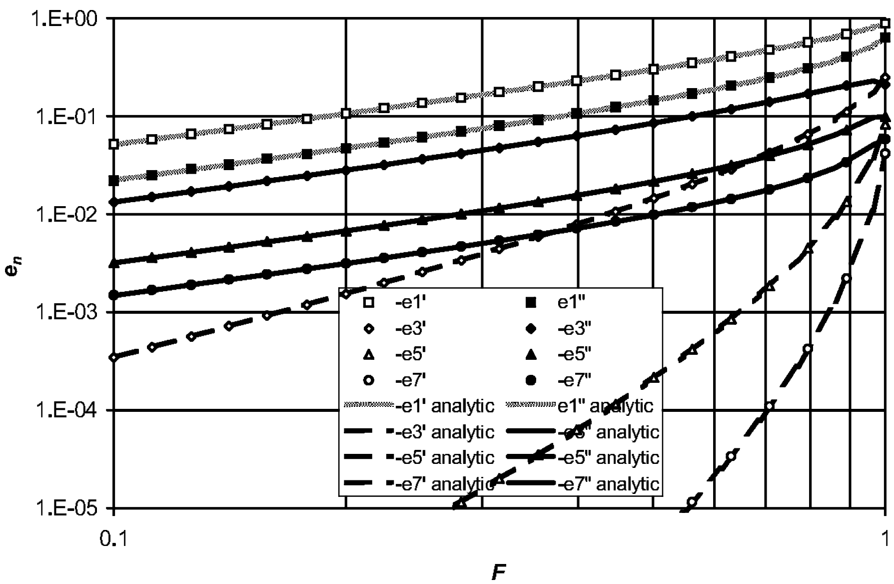

Fig. 2 Harmonic components of the voltage from Fig. 1. Dashed quantities in the legend mean the cosine parts and double-dashed the sine ones. Symbols were calculated by numerical integration, while the lines represent the analytical formulas.

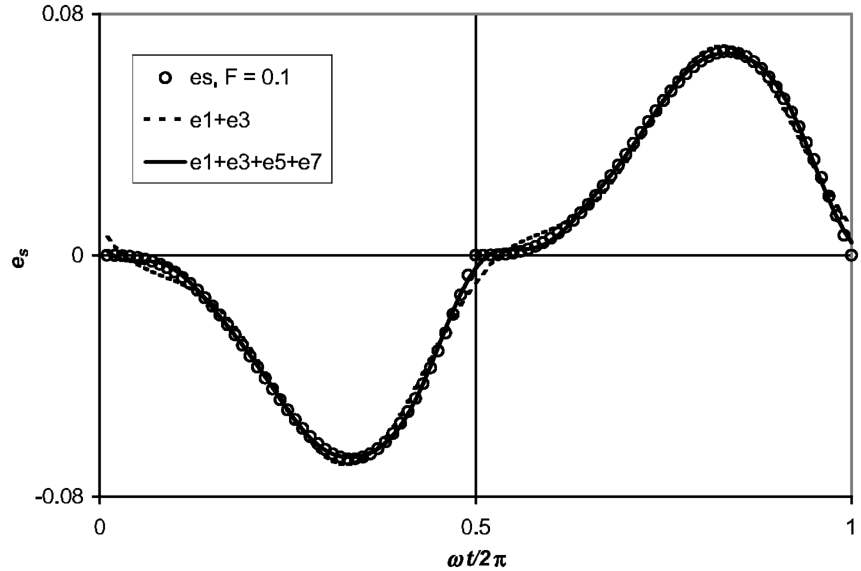

Fig. 3 Comparison of the voltage waveform at low current, with the harmonic synthesis from a limited number of components.

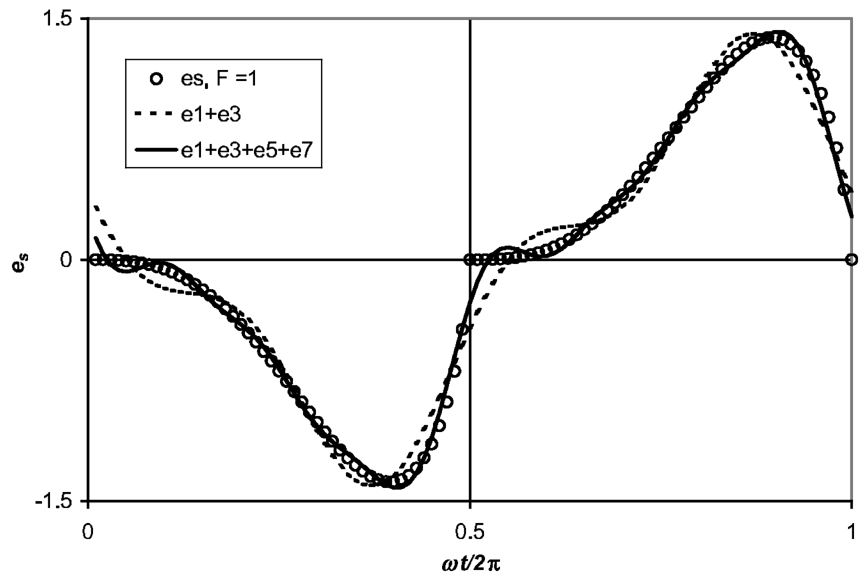

Fig. 4 Comparison of the voltage waveform at the AC current amplitude just equal to the critical current. Limitation of harmonic synthesis using the first seven harmonics is obvious.